Hindawi
Journal of Electrical and Computer Engineering
Volume 2018, Article ID 2436472, 10 pages
https://doi.org/10.1155/2018/2436472

*Research Article*

# A Detection Algorithm for the BOC Signal Based on Quadrature Channel Correlation

**Bo Qian, Guolei Zheng, and Yongxin Feng**

*School of Information Science and Engineering, Shenyang Ligong University, Shenyang 110159, China*

Correspondence should be addressed to Yongxin Feng; fengyongxin@263.net

Received 31 October 2017; Revised 11 February 2018; Accepted 22 February 2018; Published 1 April 2018

Academic Editor: Iickho Song



In order to solve the problem of detecting a BOC signal, which uses a long-period pseudo random sequence, an algorithm is presented based on quadrature channel correlation. The quadrature channel correlation method eliminates the autocorrelation component of the carrier wave, allowing for the extraction of the absolute autocorrelation peaks of the BOC sequence. If the same lag difference and height difference exist for the adjacent peaks, the BOC signal can be detected effectively using a statistical analysis of the multiple autocorrelation peaks. The simulation results show that the interference of the carrier wave component is eliminated and the autocorrelation peaks of the BOC sequence are obtained effectively without demodulation. The BOC signal can be detected effectively when the SNR is greater than −12 dB. The detection ability can be improved further by increasing the number of sampling points. The higher the ratio of the square wave subcarrier speed to the pseudo random sequence speed is, the greater the detection ability is with a lower SNR. The algorithm presented in this paper is superior to the algorithm based on the spectral correlation.

## 1. Introduction

The Binary Offset Carrier (BOC) signal is used in the global navigation satellite system (GNSS) and is characterized by multiple peaks in its autocorrelation function and spectrum splitting [1–3]. By using a square wave to modulate again, the synchronization precision of the BOC signal is improved and the interference of the same-frequency signals is decreased [4]. On the other hand, there are multiple side-peaks around the main peak of autocorrelation function of the BOC sequence, thus causing the ambiguity problem. To deal with the problem, several unambiguous techniques have been proposed [5, 6]. A novel cancellation technique of correlation side-peaks is proposed, by employing a combination of the subcorrelations making up the BOC autocorrelation [6].

The pseudo random sequence of the BOC signal has the characteristics of pseudo randomness and infinite periods in a short time, which is used in secret communications. Therefore, it is difficult to detect a BOC signal under non-cooperative conditions. In addition, by utilizing the direct sequence spread spectrum (DSSS), the BOC signal can be transmitted under a negative signal to noise ratio (SNR) and because the anti-interception ability is strong, it is more difficult to detect the signal.

To date, new methods of BOC signal recognition and parameter estimation have been proposed [7–11]. The detection methods are based on spectral correlation [7–9] and the methods for parameter estimation are based on autocorrelation [10, 11]. The basis of the spectral correlation methods is based on the cyclostationary characteristic of the BOC signal, so that the parameters of the carrier, square wave, and pseudo random sequence can be estimated. However, when the pseudo random sequence has an infinite period in a short time, the methods based on spectral correlation cannot work effectively.

The autocorrelation methods are based on the characteristics of the multiple autocorrelation peaks of the BOC signal. Based on demodulating the BOC signal, the parameters can be estimated effectively based on how the BOC signal correlates with the multiple autocorrelation peaks. Considering that the BOC signal is transmitted under a negative SNR in secret communications, demodulation is not easily achieved; therefore, it is difficult to estimate the parameters in a real-life environment.

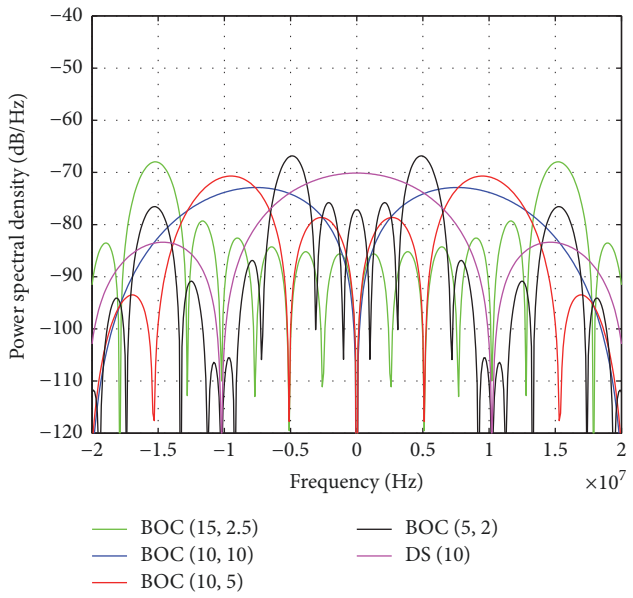


FIGURE 1: Power spectral density of the BOC signals.

In this paper, an algorithm for detecting the BOC signal is presented, using a long-period pseudo random sequence. The autocorrelation component of the carrier wave in the BOC signal is eliminated based on quadrature channel correlation. By detecting the autocorrelation peaks, the BOC signal can be detected.

The outline of this paper is as follows. In Section 2, we study the characteristics of the BOC signal. Section 3 describes the analysis of the characteristics of the multiple autocorrelation peaks for the BOC signal and the algorithm for detecting the BOC signal. Section 4 provides simulation results demonstrating the performance of the algorithm. Finally, Section 5 presents our conclusions and final comments.

## 2. Characteristics of the BOC Signal

The BOC signal $Y(t)$, modulated by BPSK, is given by

$$Y(t) = A \cdot D(t) P(t) S_c(t) \cos(2\pi f t + \varphi), \quad (1)$$

where $A$ is the carrier amplitude, $D(t)$ is the baseband data, $P(t)$ is the pseudo random sequence, $S_c(t)$ is the square wave, $f$ is the carrier frequency, and $\varphi$ is the phase. The frequency of $P(t)$ is $f_c$, and the frequency of $S_c(t)$ is $f_s$.

Firstly, the spread spectrum sequence is obtained by XOR baseband data with the pseudo random sequence. Then, the spread spectrum sequence is XORed again with a square wave to generate the BOC sequence. Finally, the BOC signal is generated by modulating the BOC sequence to the main carrier. The BOC signal is denoted as BOC $(N_s, N_c)$, where $N_s$ means the ratio of $f_s$ to the reference frequency $f_{\text{base}}$, and $N_c$ means the ratio of $f_c$ to the reference frequency $f_{\text{base}}$. In GNSS systems, the reference frequency $f_{\text{base}} = 1.023$ MHz.

The normalized power spectral density (PSD) of the BOC signal can be expressed as [12]

$$G_{\text{BOC}(f_s,f_c)}(f) = \begin{cases} f_c \left[\dfrac{\sin(\pi f/2f_s)\sin(\pi f/f_c)}{\pi f \cos(\pi f/2f_s)}\right]^2, & n \text{ is an odd number} \\ f_c \left[\dfrac{\sin(\pi f/2f_s)\cos(\pi f/f_c)}{\pi f \cos(\pi f/2f_s)}\right]^2, & n \text{ is an even number,} \end{cases} \quad (2)$$

where

$$n = \frac{2f_s}{f_c}. \quad (3)$$

The distribution of the normalized power spectral density for the BOC signals is shown in Figure 1, where DS (10) is the normalized power spectral density of the DSSS signals, in which the frequency of the pseudo random sequence is ten times as much as $f_{\text{base}}$.

As shown in Figure 1, the main lobe energy of the BOC signal is split into two lobes located at $\pm f_s$ from the central frequency. The main lobe energy of the DSSS signal is concentrated in the central frequency. Therefore, the BOC signal and the DSSS signal can be transmitted on the same frequency at the same time without interfering with each other and the bandwidth efficiency is greatly improved. Because of the wider bandwidth, the BOC signal has a greater antijamming capability than the DSSS signal. Furthermore, it is difficult to estimate the carrier frequency of the BOC signal because the two lobes are not located in the carrier frequency.

The autocorrelation function of the BOC sequence can be expressed as [13]

$$R_{\text{BOC}}(\tau) = \begin{cases} 1, & \tau = 0 \\ (-1)^{l-1}\dfrac{[n-(l-1)]}{n} + (-1)^l [4f_s - f_c(2l-1)] \cdot \left(\tau - \dfrac{l-1}{2f_s}\right), & \dfrac{(l-1)}{2f_s} < \tau \le \dfrac{l}{2f_s} \\ & 0 < l \le n-1,\ l \text{ is integer} \\ (-1)^l \dfrac{[n-|l|]}{n} + (-1)^{|l|-1} [4f_s - f_c(2|l|-1)] \cdot \left(\tau + \dfrac{|l|}{2f_s}\right), & \dfrac{|l|}{2f_s} < \tau \le \dfrac{(|l|-1)}{2f_s} \\ & -n+1 \le l < 0,\ l \text{ is integer} \\ -\dfrac{1}{N}, & T_c < |\tau| \le (N-1)T_c, \end{cases} \quad (4)$$

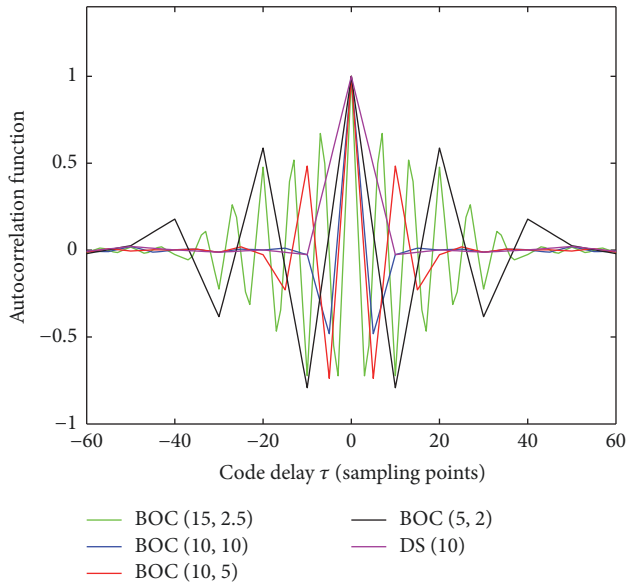


Figure 2: Autocorrelation function of the BOC sequence.

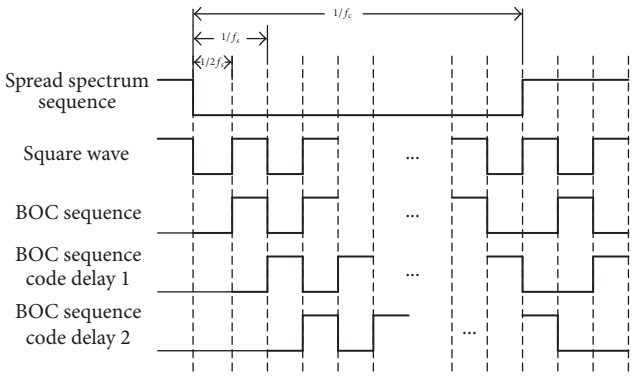


Figure 3: The generation process of the autocorrelation peaks.

where $N$ is the chip number of the pseudo random sequence in one period and $T_c$ is the period of the pseudo random sequence.

The autocorrelation functions of the BOC sequence are shown in Figure 2.

Figure 2 shows that the autocorrelation function of the BOC sequence contains multiple positive and negative peaks. The absolute values of the multiple peaks decrease gradually as the code delay increases. The sum of the multiple peaks is $2n - 1$. The width of the autocorrelation function's main peak is narrower so that the BOC sequence has a better synchronous precision. The BOC sequence is highly correlated with itself. The autocorrelation function of the DSSS sequence contains only one peak and the main peak of the DSSS sequence is wider than the peak of the BOC sequence.

As shown in Figures 1 and 2, the BOC signal has two characteristics splitting spectrum peaks and multiple autocorrelation peaks, which enhance the antijamming ability and improve the precision of the acquisition [14, 15]. In addition, the BOC signal can be transmitted with other signals, greatly improving the bandwidth efficiency [16]. The advantages of the BOC signal make it highly suitable for secret communications. However, because the main lobe energy of the BOC signal is not concentrated in the carrier frequency and the BOC signal should be transmitted under the condition of a negative SNR [17, 18], it will be difficult to estimate the carrier frequency of the BOC signal. In addition, the BOC sequence, which is commonly used in secret communications, has a longer period or is aperiodic in a short time, which increases the difficulty of detecting and estimating the BOC signal.

## 3. The Recognition Algorithm for the BOC Signal

*3.1. Multiple Autocorrelation Peaks Analysis.* The multiple autocorrelation peaks are a unique feature of the BOC sequence and can be used to detect the BOC signal. This feature is needed to analyze the relevance between the multiple autocorrelation peaks. Figure 3 shows the generation process of an unambiguous autocorrelation function for the BOC sequence.

The spread spectrum sequence, which is obtained by the XOR baseband data with the pseudo random sequence is XORed again with a square wave to generate the BOC sequence (Figure 3). Then, the BOC sequence is shifted as the code delay $\tau$ increases. When $\tau$ equals half a period of a square wave, it represents the BOC sequence code delay 1. Similarly, when $\tau$ equals one period of a square wave, it represents the BOC sequence code delay 2 (Figure 3).

When $\tau$ is 0, the normalized autocorrelation result of the BOC sequence is 1. The result of the normalized autocorrelation function decreases gradually with the increase in the code delay $\tau$ from 0 to $1/2f_s$. This represents the main peak of the autocorrelation function of the BOC sequence when $\tau = 0$ as shown in Figure 2. When $\tau$ is equal to $1/2f_s$, the phase of the square wave component in the BOC sequence 1 is inverted. As a result, the autocorrelation result of the square wave component is –1. This represents the first negative peak when $\tau = 1/2f_s$ as shown in Figure 2. With an increase in the code delay $\tau$, when $\tau$ is $1/f_s$, the phase of the square wave component in the BOC sequence 2 is the same as in the BOC sequence. As a result, the autocorrelation result of the square wave component is equal to 1. This represents the second positive peak when $\tau = 1/f_s$ as shown in Figure 2.

By parity of reasoning, because the autocorrelation result of the square wave component is changed repeatedly from 1 to –1, there are multiple positive and negative peaks in the autocorrelation function of the BOC sequence. The peaks occur at the moment when $\tau$ is the integral multiple of $1/2f_s$ and $\tau$ is less than $1/f_c$. The number of peaks is related to $f_c$ and $f_s$ and is equal to $2n-1$ with $|\tau| \le 1/f_c$ by lead and lag. When $\tau$ exceeds one chip of the pseudo random sequence, the autocorrelation result of the pseudo random sequence is $-1/N$, as shown in (3). When the period of the BOC sequence is longer or aperiodic, the autocorrelation result is nearly equal to 0.

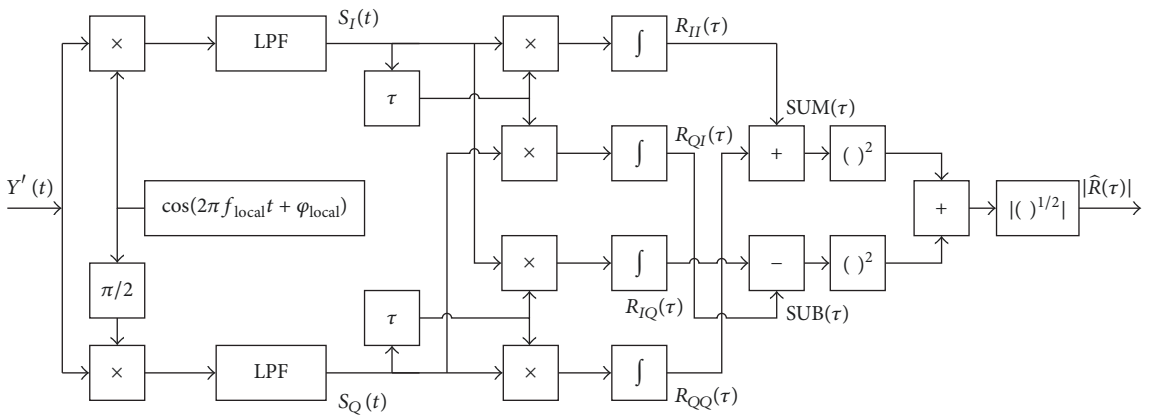


Figure 4: The overall process of the quadrature channel correlation.

By analyzing the generation process of the autocorrelation function for the BOC sequence, the values of the autocorrelation peaks can be expressed by

$$h(l) = \frac{(-1)^l (n - |l|)}{n}, \quad l = 0, \pm 1, \ldots, \pm n - 1, \tag{5}$$

where $h(l)$ is the value of the $l$-th peaks and $l$ is the sequence number of the peaks.

When $l$ is equal to 0, $h(0)$ is the value of the main peak. $l$ is positive when $\tau > 0$; otherwise it is negative. The values of the peaks decrease gradually as $|l|$ increases. Further, it is seen from (4) that the height difference between the $l$-th peak and the $(l + 1)$-th peak can be represented as

$$|\Delta h| = \left| \frac{(n - |l|)}{n} - \frac{(n - |l + 1|)}{n} \right| = \frac{1}{n}, \tag{6}$$

where $\Delta h$ is the height difference.

Because the peaks always occur at the moment when $\tau$ is the integral multiple of $1/2f_s$, the lag difference between the $l$-th peak and the $(l+1)$-th peak is $1/2f_s$. It can be represented as

$$\Delta\tau = \frac{1}{2f_s}, \tag{7}$$

where $\Delta\tau$ is the lag difference.

As shown in (5) and (6), the heights and lags of the multiple autocorrelation peaks are related to $1/2f_s$. The reason is mainly due to the second modulation by the square wave. Therefore, we can detect the BOC signal by detecting multiple autocorrelation peaks of the BOC sequence. If the relevant rules shown in (5) and (6) are satisfied, the BOC signal will be detected.

*3.2. Quadrature Channel Correlation.* Because the BOC signal is transmitted under the condition of a negative SNR and there is a carrier wave component in the BOC signal, it is difficult to obtain multiple autocorrelation peaks of the BOC sequence.

An improved method based on quadrature channel correlation is presented to obtain multiple autocorrelation peaks. The overall process of the quadrature channel correlation is shown Figure 4.

The received BOC signal can be expressed as

$$Y'(t) = A \cdot P'(t) S_c(t) \cos(2\pi f t + \varphi) + n(t), \tag{8}$$

where $P'(t)$ is the spread spectrum sequence $P'(t) = D(t)P(t)$ and $n(t)$ is the zero-mean gauss white noise with a two-sided power spectral density $N_0$.

Firstly, $Y'(t)$ is multiplied by $\cos(2\pi f_{\text{local}}t + \varphi_{\text{local}})$ and $\sin(2\pi f_{\text{local}}t + \varphi_{\text{local}})$, respectively, where $f_{\text{local}}$ is the frequency of the local oscillator and $\varphi_{\text{local}}$ is the phase of the local oscillator.

Next, the high-frequency components are filtered by a low-pass filter. We obtain

$$S_I(t) = \frac{A}{2} \cdot P'(t) S_c(t) \cos[2\pi\Delta f t + \Delta\varphi] + n_I(t) \tag{9}$$

$$S_Q(t) = -\frac{A}{2} \cdot P'(t) S_c(t) \sin[2\pi\Delta f t + \Delta\varphi] + n_Q(t), \tag{10}$$

where $\Delta f = f - f_{\text{local}}$, $\Delta\varphi = \varphi - \varphi_{\text{local}}$, and $n_I(t)$ and $n_Q(t)$ are the noise components in the $I$ and $Q$ channels after filtering.

Subsequently, the autocorrelation functions of $S_I(t)$ and $S_Q(t)$ are calculated with the code delay $\tau$. We take $S_I(t)$ as an example to study the autocorrelation and cross-correlation functions. The autocorrelation function of $S_I(t)$ can be expressed as

$$R_{II}(\tau) = R_{S_I S_I}(\tau) + R_{S_I n_I}(\tau) + R_{n_I n_I}(\tau), \tag{11}$$

where $R_{S_I S_I}(\tau)$ is the autocorrelation component of the BOC signal, $R_{S_I n_I}(\tau)$ is the cross-correlation component between the BOC signal and the noise, and $R_{n_I n_I}(\tau)$ is the autocorrelation component of the noise.

Because there is no correlation between the noise and the BOC signal, $R_{S_I n_I}(\tau)$ is nearly equal to 0 with enough received data. Then, formula (10) can be expressed as

$$R_{II}(\tau) = R_{S_I S_I}(\tau) + R_{n_I n_I}(\tau) \tag{12}$$

based on the assumption,

$$R_{n_I n_I}(\tau) \approx N_0 \delta(\tau). \tag{13}$$

The autocorrelation function $R_{S_I S_I}(\tau)$ of the BOC signal in $I$ channel can be expressed as

$$R_{S_I S_I}(\tau) = \frac{1}{2T}\lim_{T\to\infty}\int_{-T}^{T} S_I(t)\, S_I(t+\tau)\, dt = \frac{1}{2T} \cdot \lim_{T\to\infty}\int_{-T}^{T} \frac{A^2}{8} R_{\mathrm{PS}}(\tau)\cdot\cos\left[2\pi\Delta f\,(2t+\tau)+2\Delta\varphi\right] dt + \frac{A^2}{8}\cdot\cos\left(2\pi\Delta f\tau\right)\cdot R_{\mathrm{PS}}(\tau), \quad (14)$$

where

$$R_{\mathrm{PS}}(\tau) = P'(t)\, S_c(t)\, P'(t+\tau)\, S_c(t+\tau) \quad (15)$$

is the autocorrelation function of the BOC sequence.

Then, $R_{II}(\tau)$ can be expressed as

$$R_{II}(\tau) = \frac{1}{2T} \cdot \lim_{T\to\infty}\int_{-T}^{T} \frac{A^2}{8} R_{\mathrm{PS}}(\tau)\cdot\cos\left[2\pi\Delta f\,(2t+\tau)+2\Delta\varphi\right] dt + \frac{A^2}{8}\cos\left(2\pi\Delta f\tau\right)\cdot R_{\mathrm{PS}}(\tau) + R_{n_I n_I}(\tau). \quad (16)$$

Similarly, the autocorrelation function of the $Q$ channel and the cross-correlation function of the two channels are represented as

$$R_{QQ}(\tau) = -\frac{1}{2T} \cdot \lim_{T\to\infty}\int_{-T}^{T} \frac{A^2}{8} R_{\mathrm{PS}}(\tau)\cdot\cos\left[2\pi\Delta f\,(2t+\tau)+2\Delta\varphi\right] dt + \frac{A^2}{8}\cos\left(2\pi\Delta f\tau\right)\cdot R_{\mathrm{PS}}(\tau) + R_{n_Q n_Q}(\tau) \quad (17)$$

$$R_{IQ}(\tau) = -\frac{1}{2T} \cdot \lim_{T\to\infty}\int_{-T}^{T} \frac{A^2}{8} R_{\mathrm{PS}}(\tau)\cdot\sin\left[2\pi\Delta f\,(2t+\tau)+2\Delta\varphi\right] dt - \frac{A^2}{8}\sin\left(2\pi\Delta f\tau\right)\cdot R_{\mathrm{PS}}(\tau) + R_{n_I n_Q}(\tau) \quad (18)$$

$$R_{QI}(\tau) = -\frac{1}{2T} \cdot \lim_{T\to\infty}\int_{-T}^{T} \frac{A^2}{8} R_{\mathrm{PS}}(\tau)\cdot\sin\left[2\pi\Delta f\,(2t+\tau)+2\Delta\varphi\right] dt + \frac{A^2}{8}\sin\left(2\pi\Delta f\tau\right)\cdot R_{\mathrm{PS}}(\tau) + R_{n_Q n_I}(\tau). \quad (19)$$

According to (15)~(18), we obtain

$$\mathrm{SUM}(\tau) = R_{II} + R_{QQ} = \begin{cases} \frac{A^2}{4}\cos\left(2\pi\Delta f\tau\right)\cdot R_{\mathrm{PS}}(\tau), & \tau \neq 0 \\ \frac{A^2}{4} + N_0, & \tau = 0 \end{cases} \quad (20)$$

$$\mathrm{SUB}(\tau) = R_{QI} - R_{IQ} = \begin{cases} \frac{A^2}{4}\sin\left(2\pi\Delta f\tau\right)\cdot R_{\mathrm{PS}}(\tau), & \tau \neq 0 \\ 0, & \tau = 0, \end{cases} \quad (21)$$

$$\widehat{R}^2(\tau) = \mathrm{SUM}^2(\tau) + \mathrm{SUB}^2(\tau) = \begin{cases} \frac{A^4}{16} R_{\mathrm{PS}}^2(\tau), & \tau \neq 0 \\ \frac{A^4}{16} + \frac{A^2}{2} N_0 + N_0^2, & \tau = 0. \end{cases} \quad (22)$$

Then, the absolute value of the normalized multiple autocorrelation peaks is obtained as shown in the following:

$$\left|\widehat{R}(\tau)\right| = \sqrt{\widehat{R}^2(\tau)} \quad (23)$$

By using the quadrature channel correlation, the autocorrelation of the carrier component in the BOC signal has been eliminated and the multiple autocorrelation peaks of the BOC sequence are extracted.

*3.3. Detection of the Autocorrelation Peaks.* In order to detect the BOC modulation signal, it is necessary to detect the autocorrelation peaks. By analyzing multiple autocorrelation peaks of the BOC sequence as described in Section 2, we know that the heights and lags of the multiple autocorrelation peaks for the BOC sequence are related to $1/2f_s$ and that the sum of the multiple autocorrelation peaks is related to $f_c$ and $f_s$.

The absolute values of the normalized multiple autocorrelation peaks for the BOC sequence with different $f_c$ and $f_s$ values are shown in Figure 5. The sampling frequency is 400 times larger than for $f_{\mathrm{base}}$.

The frequency of the square wave should be larger than the frequency of the pseudo random sequence to generate the BOC signal. In Figure 5, the number of peaks for the BOC (10, 10) signal is two with a gradual increase in $\tau$ from 0 to $1/f_c$. The main peak appears when $\tau = 0$ and the secondary peak appears at the 20th sample point. Because one period of the square wave or the pseudo random sequence is sampled 40 times, when $\tau$ equals 20 sample points, the normalized autocorrelation result of the square wave is equal to −1. At the same time, the normalized autocorrelation result of the spread spectrum sequence is equal to 0.5 and the height of the secondary peak is equal to 0.5. When $\tau$ exceeds 40 sample points, the autocorrelation result of the spread spectrum sequence is nearly equal to 0 and there is no peak.

For the BOC (10, 5) signal, the frequency of the square wave is twice as much as the frequency of the pseudo random

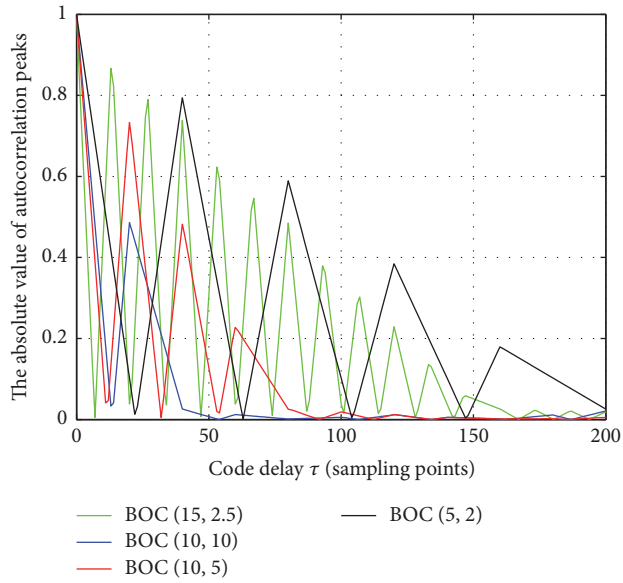


Figure 5: The absolute values of the autocorrelation peaks for the BOC sequence.

sequence. One period of the square wave is sampled 40 times and one chip of the pseudo random sequence is sampled 80 times. When $\tau$ equals 20 sample points, the normalized autocorrelation result of the square wave is equal to −1. At the same time, the normalized autocorrelation result of the square wave is equal to 0.75. Therefore, the absolute value of the normalized autocorrelation result for the BOC sequence is equal to 0.75. This represents the secondary peak. When $\tau$ equals 40 sample points, it represents the third peak and the height of the peak is equal to 0.5. The last peak occurs at 60 sample points and the height of the peak is equal to 0.25. There is no peak when $\tau$ exceeds 80 sample points. Similarly, for the BOC (5, 2) signal, the secondary peak occurs at 40 sample points and the height of the peak is equal to 0.8. For the BOC (15, 2.5) signal, the secondary peak occurs at 13 sample points and the height of the peak is equal to 0.87.

By analyzing the multiple autocorrelation peaks of the BOC sequence described in Section 2.1 and Figure 5, the secondary peak occurs at the moment that $\tau$ equals half a period of the square wave. Therefore, when $f_c$ is equal to $f_s$, the height of the secondary peak is equal to 0.5. When $f_s$ is larger than $f_c$, the height of the secondary peak is larger than 0.5, as shown in Figure 5. With a gradual increase in $\tau$, the heights of the peaks decrease gradually. Because $f_s$ is not less than $f_c$, the height of the secondary peak is not less than 0.5. Therefore, the initial threshold for detecting the secondary peaks can be equal to 0.5. The secondary peak is determined by the absolute value of the normalized autocorrelation result, which is the largest peak except for the main peak and it is not less than 0.5. If there is no peak, it is not a BOC signal. Otherwise, according to the height and lag difference, $\Delta h$ and $\Delta\tau$ can be estimated. We can determine the next peak with $\Delta h$ and $\Delta\tau$ until the height is nearly equal to 0. If there are multiple peaks, this means it is a BOC signal.

As shown in (21), there is an autocorrelation component of the noise in $y(\tau)$ with $\tau = 0$. When the SNR is low, the autocorrelation component of the noise is large, which will lead to greater errors for $\Delta h$, and this has a large impact on the ability to detect the BOC signal. Therefore, the absolute values of the normalized multiple autocorrelation peaks need to be adjusted. Based on the least squares fitting method, the autocorrelation results that are close to the main peak and are descending continuously are determined and the height of the main peak is adjusted.

The flow of the algorithm is shown in Figure 6.

## 4. Simulation Results

We assume the following parameters for the simulations: $f_c$ = 2.046 MHz, $f_s$ = 5.115 MHz, $f_s$ = 20.46 MHz, and $f_{\text{local}}$ = 10.23 MHz. The sampling frequency is 204.6 MHz and the number of sampled points is 25000.

Figure 7 shows the absolute values of the autocorrelation peaks for the BOC (5, 2) signal with SNR = 10 dB. It is evident that the autocorrelation component of the carrier wave is eliminated by using the quadrature channel correlation. The multiple autocorrelation peaks are easy to detect. For the absolute values of the normalized multiple autocorrelation peaks (without the elimination of the autocorrelation component of the carrier wave), there are more peaks that are caused by the carrier autocorrelation around the peaks of the BOC sequence. This can interfere with the detection of the peaks. From Figure 7, we can see that the multiple autocorrelation peaks of the BOC sequence are obtained by the quadrature channel correlation and the BOC signal does not require demodulation.

Figure 8 shows the absolute values of the autocorrelation peaks for the BOC (5, 2) signal with different SNR values. Because there is a noise autocorrelation component that is

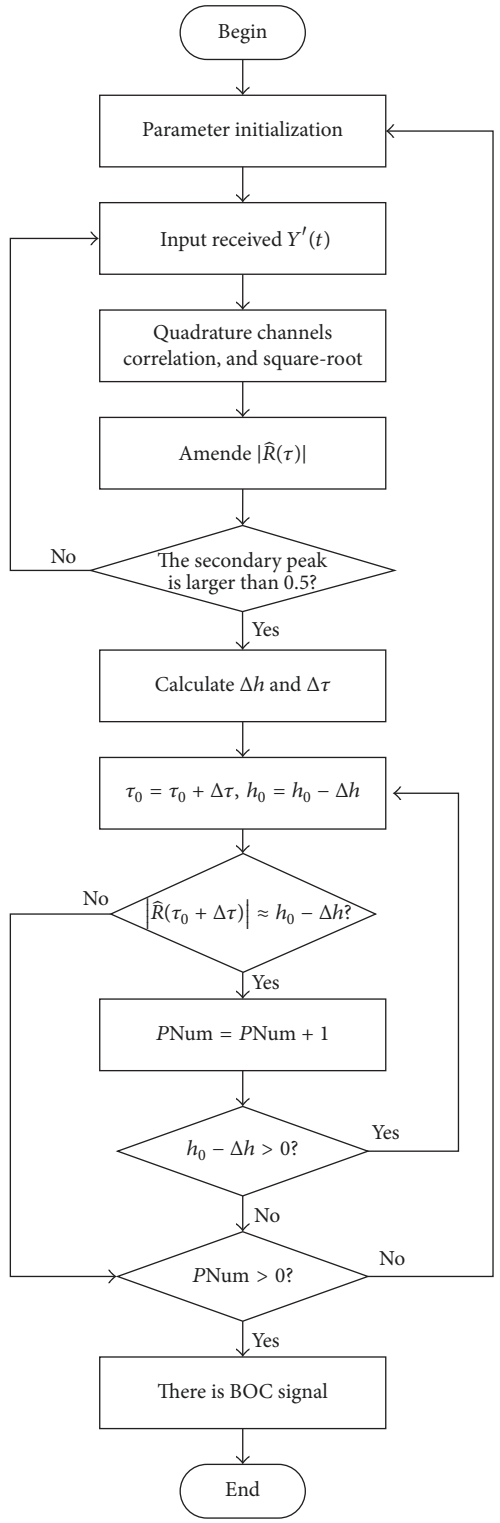


Figure 6: Flowchart of the proposed algorithm.

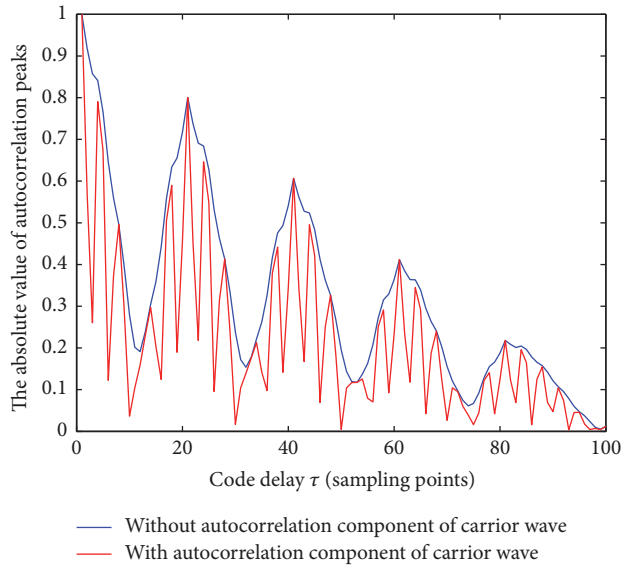


Figure 7: The absolute value of the autocorrelation peaks with SNR = 10 dB.

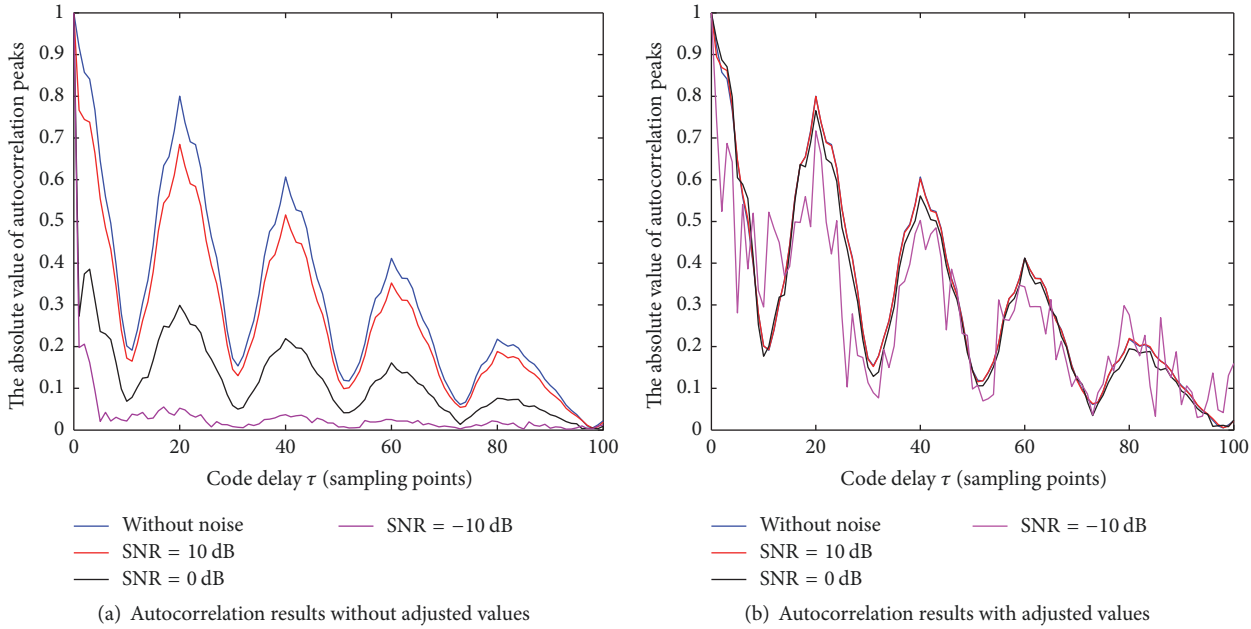


Figure 8: The absolute value of the autocorrelation peaks with different SNR.

included in the main peaks as shown in (a), the main peaks increase as the SNR gradually decreases. Therefore, the other normalized autocorrelation peaks are lower with a lower SNR such as the secondary peak and the third peak. The noise autocorrelation component in the main peak is eliminated after the adjustment. As a result, the adjusted result for the multiple peaks is similar to the result under a noise-free condition.

Table 1 shows the results for the detection of the multiple peaks. It is evident that the heights of the peaks decrease gradually as $\tau$ increases. For SNR = 10 dB, there are the approximate height differences $\Delta h$ and lag differences $\Delta\tau$ between the adjacent peaks. For lower values of the SNR, the error gradually increases.

Figure 9 shows the performance of the proposed algorithm for different data lengths. When the data length is 25000, the BOC (5, 2) signal can be detected effectively when the SNR is greater than −12 dB. When the data length is 100000, the detection probability of the BOC (5, 2) signal increases to 1 dB. The detection performance for the BOC (5, 2) signal can be improved with an increase in the data length because the autocorrelation component of the noise is smaller with a greater data length. Therefore, the detection ability of the proposed algorithm is higher at a lower SNR. However,

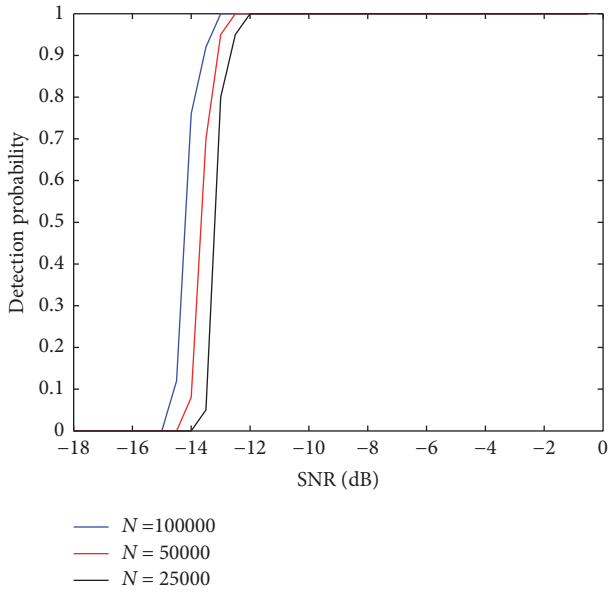


Figure 9: Detection probability with different data lengths.

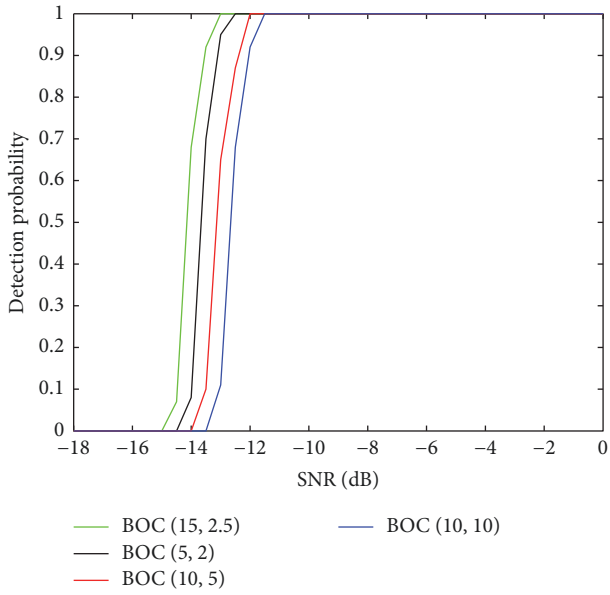


Figure 10: Detection probability for different values of $f_c$ and $f_s$.

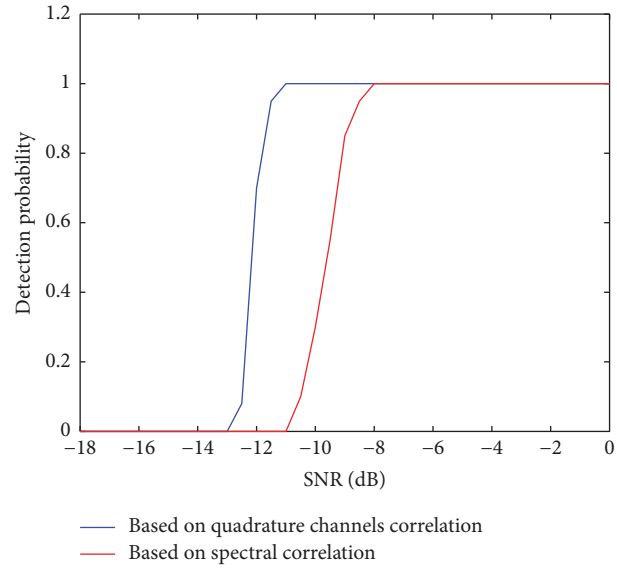


Figure 11: Detection probability for different algorithms.

Table 1: The results of the peak detection.

| SNR/dB | Number of peaks | Height | $\tau$/sampled points | $\Delta h$ |
|---|---|---|---|---|
| 10 dB | 1 | 1 | 0 | 0 |
| | 2 | 0.7992 | 20 | 0.2008 |
| | 3 | 0.6021 | 40 | 0.1971 |
| | 4 | 0.4122 | 60 | 0.1899 |
| | 5 | 0.2197 | 80 | 0.1925 |
| 0 dB | 1 | 1 | 0 | 0 |
| | 2 | 0.7655 | 20 | 0.2345 |
| | 3 | 0.5613 | 40 | 0.2042 |
| | 4 | 0.4122 | 60 | 0.1491 |
| | 5 | 0.195 | 80 | 0.2172 |
| −10 dB | 1 | 1 | 0 | 0 |
| | 2 | 0.7173 | 20 | 0.2827 |
| | 3 | 0.5025 | 40 | 0.2148 |
| | 4 | 0.3473 | 59 | 0.1552 |
| | 5 | 0.2984 | 79 | 0.0489 |

when the SNR is lower than −15 dB, the BOC signal cannot be detected when the data length is 100000.

Figure 10 shows the performance of the proposed algorithm for different values of $f_c$ and $f_s$ with a data length of 100000. When the ratio $n$ of $f_s$ to $f_c$ is larger, the probability of detecting the BOC signal is higher for the same SNR because there are more peaks with a larger $n$ and the height of the secondary peak is larger. Therefore, it is easy to detect the peaks and detect the BOC signal.

Figure 11 shows the performance of the proposed algorithm based on the quadrature channel correlation and the spectral correlation. It is evident that the probability of detecting the BOC signal is higher for the quadrature channel correlation than for the spectral correlation algorithm. Under the same conditions, the detection probability for the BOC signal is improved by about 2 dB.

## 5. Conclusions

(1) The autocorrelation component of the carrier wave is eliminated by using the quadrature channel correlation. If the adjacent autocorrelation peaks have the same lag differences and height differences, the BOC signal is detected effectively by detecting the absolute value of the multiple autocorrelation peaks.

(2) The ability to detect the BOC signal is related to the data length and the ratio of $f_s$ to $f_c$. Larger values for the data length and the ratio of $f_s$ to $f_c$ result in a higher probability to

detect the BOC signal. The algorithm presented in this paper is superior to the algorithm based on the spectral correlation.

## Conflicts of Interest

The authors declare that there are no conflicts of interest regarding the publication of this paper.

## Acknowledgments

This work is supported by the Science and Technology Foundation from Liaoning Education Department (no. L2015462), Shenyang Ligong University Liaoning Province Information Network and Countermeasure Technology Key Laboratory Open Foundation (2015), and Shenyang Ligong University Postdoctoral Science Foundation.

## References

[1] M. Foucras, J. Leclère, C. Botteron et al., "Study on the cross-correlation of GNSS signals and typical approximations," *GPS Solutions*, vol. 21, no. 2, pp. 293–306, 2017.

[2] B. Tripathi, R. Tulsian, and R. C. Jain, "Performance Comparison of Sine and Cosine Phased BOC Signals Used for Radionavigation," in *Proceedings of the IFAC*, vol. 45, pp. 223–228, 2012.

[3] K. Chae, S. R. Lee, H. Liu, and S. Yoon, "An unambiguous correlation function for generic sine-phased binary offset carrier signal tracking," *Computers and Electrical Engineering*, vol. 49, pp. 161–172, 2016.

[4] Z. Yanling, L. Xuejiao, and W. Xiaoqing, "Analysis of satellite navigation signal alternate binary offset carrier modulation," *Journal of Hubei University*, no. 4, pp. 334–339, 2015.

[5] Z. Yao, X. Cui, M. Lu, Z. Feng, and J. Yang, "Pseudo-correlation-function-based unambiguous tracking technique for sine-BOC signals," *IEEE Transactions on Aerospace and Electronic Systems*, vol. 46, no. 4, pp. 1782–1796, 2010.

[6] Y. Lee, D. Chong, I. Song, S. Y. Kim, G.-I. Jee, and S. Yoon, "Cancellation of correlation side-peaks for unambiguous BOC signal tracking," *IEEE Communications Letters*, vol. 16, no. 5, pp. 569–572, 2012.

[7] A. F. Khalaf, M. I. Owis, and I. A. Yassine, "Image features of spectral correlation function for arrhythmia classification," in *Proceedings of the 37th Annual International Conference of the IEEE Engineering in Medicine and Biology Society, EMBC '15*, pp. 5199–5202, IEEE, Milan, Italy, August 2015.

[8] T. Zhang, D. He, S. Chen, and S. Zhou, "Spectral correlation-based parameter estimation of BOC modulation signal," *Journal of Huazhong University of Science and Technology*, vol. 41, no. 9, pp. 11–16, 2013.

[9] S. Zhu, D. Zhao, and F. Wang, "Hybrid prediction and fractal hyperspectral image compression," *Mathematical Problems in Engineering*, vol. 2015, Article ID 950357, 10 pages, 2015.

[10] T. Former, "Phase clustering based modulation classification algorithm for PSK signal over wireless environment," *Mobile Information Systems*, vol. 2016, Article ID 2398464, 11 pages, 2016.

[11] R. Chen, J. Wang, R. Lin, and X. Zhao, "Spectrum sensing based on nonparametric autocorrelation in wireless communication systems under alpha stable noise," *Mobile Information Systems*, vol. 2016, Article ID 6753830, 6 pages, 2016.

[12] F. Guo, Z. Yao, and M. Lu, "BS-ACEBOC: a generalized low-complexity dual-frequency constant-envelope multiplexing modulation for GNSS," *GPS Solutions*, vol. 21, no. 2, pp. 561–575, 2017.

[13] M. S. Yarlykov, "Correlation functions of BOC and AltBOC signals as the inverse Fourier transforms of energy spectra," *Journal of Communications Technology and Electronics*, vol. 61, no. 8, pp. 857–876, 2016.

[14] M. S. Yarlykov and S. M. Yarlykova, "Correlation functions of complete CBOC signals derived as the inverse Fourier transform of energy spectra," *Journal of Communications Technology and Electronics*, vol. 62, no. 2, pp. 128–140, 2017.

[15] B. Yin, G. Wang, and Y. Qi, "Unambiguous sine-phased binary offset carrier modulated signal tracking technique," *Optik - International Journal for Light and Electron Optics*, vol. 132, pp. 284–290, 2017.

[16] P. Weichuan, W. Xue, and H. Chengyan, "Research on correlation peaks detection algorithm for multiplex signal of navigation systems," *Journal of Time and Frequency*, vol. 38, no. 3, pp. 163–170, 2015.

[17] F. Liu and Y. Feng, "A new acquisition algorithm with elimination side peak for all BOC signals," *Mathematical Problems in Engineering*, vol. 2015, Article ID 140345, 9 pages, 2015.

[18] K. Chae, S. R. Lee, H. Liu et al., "A novel unambiguous composite binary offset carrier (6, 1, 1/11) tracking based on partial correlations," *Computers and Electrical Engineering*, vol. 50, pp. 54–66, 2016.